# Deformation Effect on Proton Bubble Structure in $N = 28$ Isotones

**Pankaj Kumar**\*, **Virender Thakur, Smriti Thakur, Raj Kumar** and **Shashi K Dhiman**

*Department of Physics, Himachal Pradesh University, Shimla-171005, India*

\*pankajdhiman659@gmail.com (Corresponding Author)

## ARTICLE INFORMATION

## ABSTRACT

**Purpose:** To study the effect of nuclear deformation on proton bubble structure of $N = 28$ isotones and and compare it with the spherical limits. The reduction of depletion fraction due to deformation can be explained by studying the relative differences in the central densities.

**Methods:** In this work, we have employed relativistic Hartree-Bogoliubov (RHB) model with density-dependent meson-exchange (DD-ME2) interaction and separable pairing interaction. We have performed axially constrained calculations to investigate the deformed proton bubble structure in $^{40}$Mg, $^{42}$Si, $^{44}$S, and $^{46}$Ar, isotones of $N = 28$ shell closure.

**Results:** We have observed that the nuclear deformation play against the formation of bubble structure. In the spherical limits, the isotones of $N = 28$ shell closure have pronounced bubble structure with large value of depletion fraction. But, the increase in deformation leads to the disappearance of bubble structure. The internal densities in deformed nuclei are found to increase with deformation which can be related to the decrease in depletion fraction.

**Conclusion:** By using RHB model, we have investigated the ground state and proton bubble structure of $N = 28$ isotones. In $^{44}$S, and $^{46}$Ar, the $2s_{1/2}1d_{3/2}$ states get inverted due to the weakning of spin-orbit strength. Due to strong dynamical correlations, arising from deformation, the central depletion of proton density is greatly affected in these isotones. The decrease in depletion fraction can be related to increase in the internal density due to deformation.

## 1. Introduction

The nuclear density distribution unfolds information regarding the shape and stability of the nuclear system. The saturation property of nuclear force states that the nuclear density is constant inside the nucleus $\left(\rho_0 \approx 0.16\,fm^{-3}\right)$ irrespective of the number of nucleons. In certain cases, an interesting fact is observed in context of the nuclear density profile known as "bubble effect". The bubble effect in nuclei is characterized by the depletion of central nucleonic density with a hump nearby it. In recent years, there has been an increasing interest in the search of central depression of nucleonic density.

The possibility of central density depletion in stable spherical nuclei was firstly proposed in 1940s by H.A. Wilson [1]. In 1970s, Campi and Sprung have performed the first microscopic calculations for the spherical bubble nuclei [2]. The existence of bubble or semi-bubble structures in light, medium, and superheavy nuclei has been investigated in many studies [3-9]. In these studies, it was suggested that the shell effects are responsible for the central density depletion in light nuclei. In the superheavy region, the occurrence of bubble structure has been ascribed to Coulomb repulsion due to the movement of protons towards the nuclear surface [10-12]. Interestingly, one can found the phenomenon of bubble structure is in all mass regions.

In a nucleus, the wave function of s-orbit has a radial distribution peaked in the nuclear interior and this part of the wavefunction contributes to the central density. However, the wavefunction of orbitals with non-zero angular momenta do not contribute to central density as the peaks of these wavefunctions are suppressed by the centrifugal barrier. This means that only s-orbit contribute to the nuclear density at the center and the depopulation of this state cause the depletion of central density in the nucleus and hence a bubble may form. Such an interior peaked shape of $3\,s$ wavefunction was measured using electron scattering on $^{206}$Pb and $^{205}$Tl [3]. The emergence of a bubble structure also affects the spin-orbit potential. In bubble nuclei, the spin-orbit strength gets weaker which may cause $2s_{1/2}$-$1d_{3/2}$ orbital inversion in light nuclei [4,5]. The first experimental study of the bubble structure has been reported recently for $^{34}$Si [13]. The emptiness of $2s_{1/2}$ proton orbit was observed for $^{34}$Si observed in this experiment.

These sophisticated radioactive ion beam facilities have opened a testing ground for theoretical predictions. In the literature, most of the bubble nuclei have been explored for spherical cases. Nuclear deformation disfavors the formation of a bubble as it admix $s$ orbital with the higher $l$ orbitals [4,7,8,14,15]. The first study of axially deformed bubble nuclei in light mass region was done by Shukla et al. [16]. In our previous work, we studied the possibility of deformed dual bubble-like structure in light nuclei [17]. We found some potential candidates around $N$ or/and $Z = 14$ exhibiting a deformed dual bubble structure. The isotones of $N = 28$ shell closure are not spherical in their ground state [18]. In the present work, our purpose is to study the effect of nuclear deformation on proton bubble structure in $N = 28$ isotones.

During the past decades, the relativistic nuclear density functional theories have achieved great success in describing nuclear properties of both stable and unstable nuclei throughout the nuclear chart [19-21]. The RHB model based on Covariant density functional theory (CDFT) is one of the most attractive nuclear density functional theories to describe the ground- and excited-state properties for both spherical and deformed nuclei. In the present work, we have used the Covariant Density Functional Theory to describe the impact of deformation on proton bubble structure in $N = 28$ isotones and the phenomena behind it.

This paper is organized as follows: In Section 2, we have briefly described the outline of the RHB model with the separable pairing interaction. The results for density distributions of deformed bubble candidates and impact of deformation are presented in Section 3. Finally, the concluding remarks are given in Section 4.

## 2. Theoretical formalism

### 2.1. Meson Exchange Model

In the framework of meson-exchange model, a nucleus is described as a system of Dirac spinors which are interacting by the exchange of point-like particles, called mesons. The total Lagrangian density of mesons exchange model involves the isoscalar-scalar σ-meson, the isoscalar-vector ω-meson, and the isovector-vector ρ-meson and can be written as [22,23]:

$$\mathcal{L} = \sum_i \bar{\psi}_i \left( i\gamma_u \partial^\mu - m \right) \psi_i + \frac{1}{2} \partial_\mu \sigma \partial^\mu \sigma - \frac{1}{2} m_\sigma^2 \sigma^2$$
$$- \frac{1}{2} \Omega_{\mu\nu} \Omega^{\mu\nu} + \frac{1}{2} m_\omega^2 \omega_\mu \omega^\mu - \frac{1}{4} \vec{R}_{\mu\nu} \vec{R}^{\mu\nu}$$
$$+ \frac{1}{2} m_\rho^2 \vec{\rho}_\mu \cdot \vec{\rho}^\mu - \frac{1}{4} F_{\mu\nu} F^{\mu\nu} - g\sigma \bar{\psi}\psi\sigma$$
$$- g_\omega \bar{\psi}\gamma^\mu \psi \omega_\mu - g_\rho \bar{\psi}\vec{\tau}\gamma^\mu \psi \cdot \vec{\rho}_\mu - e\bar{\psi}\gamma^\mu \psi A_\mu, \qquad (1)$$

where the first term represent the Lagrangian of free nucleons with bare mass $m$ and ψ denotes the Dirac spinors for nucleons. $m_\sigma, m_\omega, m_\rho$ represents the masses of $\sigma, \omega$, and ρ mesons with corresponding coupling constants $g_\sigma, g_\omega, g_\rho$ for the mesons to the nucleons, respectively. $\Omega_{\mu\nu}, \vec{R}_{\mu\nu}, F_{\mu\nu}$ are field tensor of the vector fields ω, ρ, and the photon [24].

The functionals are described by density-dependent coupling constants $g_i(\rho)$ (for $i = \sigma, \omega, \delta$). The coupling of σ-meson field and ω-meson field to the nucleon field is written as, [24,25].

$$g_i(\rho) = g_i(\rho_{sat}) f_i(x) \quad \text{for } i = \sigma, \omega \qquad (2)$$

with

$$f_i(x) = a_i \frac{1 + b_i (x + d_i)^2}{1 + c_i (x + d_i)^2} \qquad (3)$$

For density dependence of ρ-meson coupling, Dirac-Brueckner calculations of asymmetric nuclear matter suggested the functional form [26], given by

$$g_\rho(\rho) = g_\rho(\rho_{sat}) e^{-a_\rho(x-1)} \qquad (4)$$

The isovector channel is parameterized by $g_\rho(\rho)$ and $a_\rho$. This model is represented in the present investigations by the parameter set DD-ME2 [22].

The inclusion of pairing correlations is important for the description of open-shell nuclei [27, 28]. In the RHB model, the mean-field and pairing correlations are treated self consistently. Here, the single-particle density matrix can be generalized in two densities, the normal density $\hat{\rho}$, and pairing tensor $\hat{\kappa}$. The RHB energy density functional is then given by

$$E_{RHB}[\hat{\rho}, \hat{\kappa}] = E_{RMF}[\hat{\rho}] + E_{pair}[\hat{k}], \qquad (5)$$

where $E_{RMF}[\hat{\rho}]$ is the nuclear energy density functional and is given by [29]

$$E_{RMF}[\psi, \bar{\psi}, \sigma, \omega^\mu, \bar{\rho}^\mu, A_\mu] = \int d^3r \mathcal{H}(r). \qquad (6)$$

The pairing part of RHB functional is given by

$$E_{pair}[\hat{\kappa}] = \frac{1}{4} \sum_{n_1 n_1'} \sum_{n_2 n_2'} \kappa^*_{n_1 n_1'} \left\langle n_1 n_1' \middle| V^{PP} \middle| n_2 n_2' \right\rangle \kappa_{n_2 n_2'}, \qquad (7)$$

where $\left\langle n_1 n_1' \middle| V^{PP} \middle| n_2 n_2' \right\rangle$ are the matrix elements of the two-body pairing interaction.

The pairing force is separable in momentum space and can be transformed from momentum to coordinate space with the form of

$$V^{PP}(r_1, r_2, r_1', r_2') = -f_p G\delta(R - R') P(r) P(r'), \qquad (8)$$

where $R = \frac{1}{\sqrt{2}}(r_1 + r_2)$ and $r = \frac{1}{\sqrt{2}}(r_1 - r_2)$ represent the center of mass and the relative coordinates, respectively and the form factor $P(r)$ is of Gaussian shape

$$P(r) = \frac{1}{\left(4\pi a^2\right)^{3/2}} e^{-r^2/2a^2}. \tag{9}$$

The factor $f_p$ is the scaling factor of the pairing force. Pairing mixes the states around the Fermi surface and the bubble formation might get suppressed. To take care of pairing effects, the value of the scaling factor is taken as $f_p = 1.0$ in the present work. The two parameters $G$ and $a$ have been adjusted to reproduce the density dependence of gap at the Fermi surface $\Delta(\kappa_F)$ in the nuclear matter [27, 30], and their values are taken as $G = 728$ MeV fm$^3$ and $a = 0.644$ fm for both protons and neutrons. The pairing force has a finite range, and also it conserves translational invariance due to the presence of the factor $\delta(R - R')$. The anti-symmetrized pp matrix elements can be represented as a sum of a finite number of separable terms in the harmonic oscillator basis

$$\langle n_1 n_2 | V^{pp} | n'_1 n'_2 \rangle a = \sum_N W^{N*}_{n_1 n_2} W^N_{n'_1 n'_2}. \tag{10}$$

The pairing field $\Delta$, in this case, takes the form

$$\Delta_{n_1 n_2} = \sum_N P_N W^{N*}_{n_1 n_2} \text{ with } P_N = \frac{1}{2} Tr\left(W^N \kappa\right), \tag{11}$$

and finally, the pairing energy in the nuclear ground state is given by

$$E_{pair} = -G \sum_N P_N^* P_N \tag{12}$$

In this work, the RHB model based on CDFT with DD-ME2 interaction is used. To understand the effect of nuclear deformation on bubble structure, we have performed axially constrained calculations. The spherically constrained calculations have also been carried out as a reference to clarify the role of deformation.

## 3. Results and Discussion

The $N = 28$ shell closure is produced by spin-orbit splitting. In light nuclei, the $N = 28$ shell gap get eroded due to the quadrupole excitations across it [31-33]. The reduction of $N = 28$ spherical shell gap towards the neutron-rich side is responsible for this erosion. Therefore, the isotones of $N = 28$ magic shell have a deformed ground state. The deformation in a nucleus mainly depends on the number of nucleons (protons and neutrons) it contain. The shape of most nonspherical nuclei is characterized by axially symmetric

quadrupole deformations (prolate or oblate). The evolution of single-nucleon shell structure is the origin of deformation in a nucleus. For these isotones ($^{40}$Mg, $^{42}$Si, $^{44}$S, and $^{46}$Ar), the values of quadrupole deformation parameter $\beta_2$ are taken from our previous work [18]. The values of deformation parameter $\beta_2$ are given in second column of Table 1.

**Table 1**: The calculated values of quadrupole deformation parameter $\beta_2$ for $N = 28$ isotones are compared with the available experimental data [35]. The last two columns shows the depletion fraction (DF) for proton bubbles corresponding to spherical solution and ground-state solution.

| Nucleus | $\beta_2$[g.s.] | $\beta_2$[Exp.] | $\beta_2 = 0$ $DF_p$(%) | $\beta_2$[g.s.] $DF_p$(%) |
|---|---|---|---|---|
| $^{40}$Mg | 0.44 | - | 31.76 | 27.73 |
| $^{42}$Si | -0.35 | - | 42.91 | 13.13 |
| $^{44}$S | 0.34 | 0.258 | 39.49 | 18.54 |
| $^{46}$Ar | -0.18 | 0.196 | 31.46 | 16.61 |

The bubble effect in the nuclei can be quantified in terms of depletion fraction (DF), given by:

$$DF = \frac{\rho_{max.} - \rho_{cen.}}{\rho_{max.}} \times 100\%, \tag{13}$$

where $\rho_{max.}$ and $\rho_{cen.}$ are maximum and central nucleon density, respectively. The bubble nuclei are characterized by a large value of DF. In $N = 28$ isotones, the unoccupancy of proton $2s_{1/2}$ orbital leads to a proton bubble structure. The formation of bubble structure is associated with the shell effects. The weak dynamical correlations between $s$-orbital and higher angular momentum orbitals ensure the bubble formation [34]. Deformation causes the mixing or overlapping of $sd$ states and leads to stronger dynamical correlations. These correlations ultimately disfavor the formation of a bubble.

Discussing the spherical limits of these isotones, a pronounced proton bubble structure is observed. Fig. 1 presents the proton single-particle energy levels for $^{40}$Mg, $^{42}$Si, $^{44}$S, and $^{46}$Ar nuclei. In $^{40}$Mg and $^{42}$Si, the proton $2s_{1/2}$ orbital is empty, as all the protons are filled in $1d_{5/2}$ orbital. While, in case of $^{44}$S and $^{46}$Ar, the $2s_{1/2}$ level become depopulated due to the inversion of $2s_{1/2}$-$1d_{3/2}$ orbitals. The value of occupation probabilities are given in the paranthese. The occupation probabilities for each spherical s.p. state are obtained by dividing those occupation numbers by the maximum occupation number $(2j+1)$ for each s.p. state. The inversion of $2s_{1/2}$-$1d_{3/2}$ orbitals can be ascribed to the weakening of spin-orbit strength.
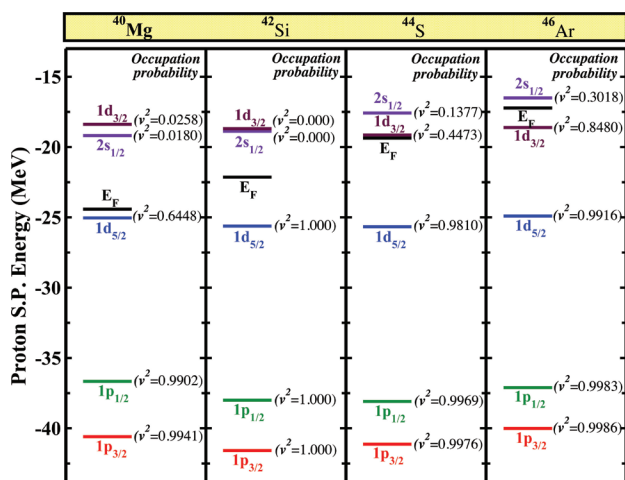
**Figure 1:** (Color online) Proton single-particle energy levels for $^{40}$Mg, $^{42}$Si, $^{44}$S, and $^{46}$Ar nuclei. The value of occupation probabilities are given in the paranthese.
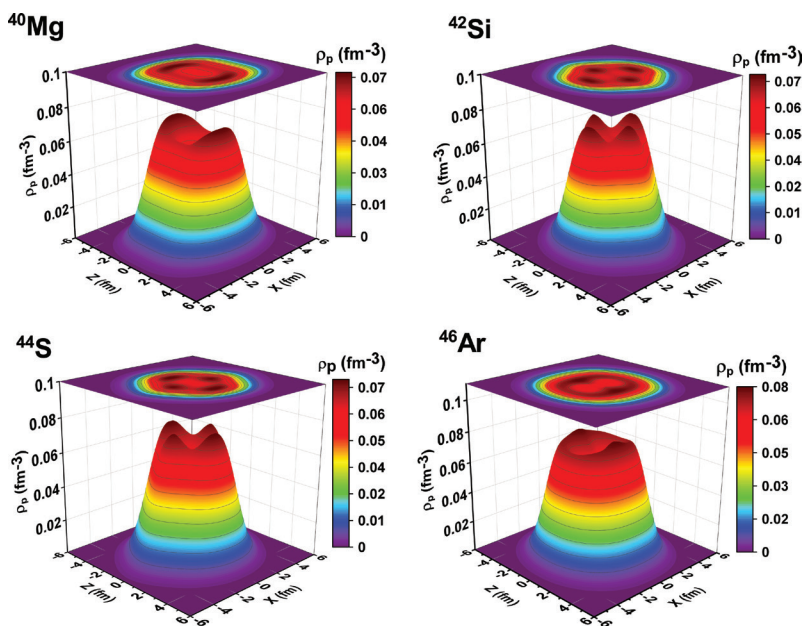
Fig. 2 presents the 3D plots of proton density profiles of deformed ground state in $^{40}$Mg, $^{42}$Si, $^{44}$S, and $^{46}$Ar. The symmetry axis is denoted by $z$ and the perpendicular axis by $x$. The depletion of central proton density can be observed in these nuclei. Also, the shape of formed proton bubbles has a substantial deformation. The characteristics of occupied s.p. orbits are necessary to determine the density distributions in the nucleus. All of these isotones are found to have a very low occupation probability of $2s_{1/2}$ orbital in their ground states. Thus, we may say that the deformation plays a predominant role in the quenching of central depletion of density than the occupancy of $2s_{1/2}$ orbital. Shell effects are high for magic spherical configurations [34]. Due to deformation, the large dynamical correlations arise due to broken $(2j+l)$ degeneracy which ultimately leads to a less pronounced shell effect and the depletion fraction decreases with the increase in deformation.



**Figure 2:** (Color online) Proton density profiles for $^{40}$Mg, $^{42}$Si, $^{44}$S, and $^{46}$Ar nuclei along symmetry axis, $z$, and coordinate axis, $x$. The dark red color corresponds to maximum density while the dark violet color to lower density or zero density.

In the case of deformed nuclei, it is significant to define axis-specific depletion fraction. The last two columns of Table 1 presents the values of proton depletion fraction for $^{40}$Mg, $^{42}$Si, $^{44}$S, and $^{46}$Ar along the symmetry axis $z$. In this table, we have shown a comparison of proton depletion fraction with the spherical mean-field solution ($\beta_2 = 0$) and ground state solution ($\beta_2[g.s.]$). A pronounced drop in depletion fraction is observed for the nuclei with large deformation. Shell effects are observed to be more pronounced for the prolate mean-field solution than the

oblate mean-field solution which can be related to the lowering of some deformed s.p. states. Thus, the nuclei with an oblate ground state have a low value of depletion fraction.

Another possible reason for the decrease in value of depletion fraction is the enhancement of central density due to deformation. To understand this, we have compared the central densities that come from the deepest single-particle orbits obtained by deformed and spherical mean-field calculations. For further investigation, we have calculated the correlation between depletion fraction and internal

density. We calculate the relative differences in the central densities ($\Delta[\rho(0)]$) obtained from deformed and spherically constrained calculations, given by [36]

$$\Delta\big[\rho(0)\big] = \frac{\big[\rho(0) - \rho^{sph.}(0)\big]}{\rho^{sph.}(0)}, \qquad (14)$$

where $\rho(0)$ denotes the central density for deformed solution and $\rho^{sph.}(0)$ shows the central density for spherical mean-field solution. Fig. 3 presents the correlation plot of the relative difference of internal densities and the depletion fraction of the deformed state for these isotones. It can be observed from Fig. 3 that internal densities in deformed nuclei increase that leads to the decrease in depletion fraction in the deformed ground state or *vice - versa*. It can also be observed that the nuclear deformation leads to an increase in the internal density of the nucleus. The other contribution may come from the change in densities of $2s_{1/2}$ orbit driven by the deformation, which is not easy to identify as it is constructed from various deformed s.p. orbits.
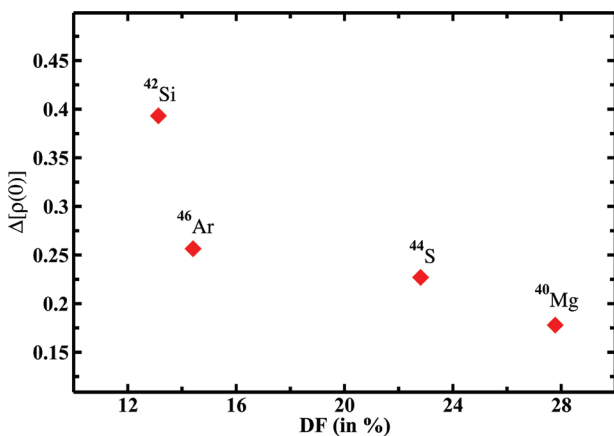


**Figure 3:** (Color online) Plot of relative differences in the internal densities versus the depletion fraction.

## 4. Conclusion

In the present study, we have investigated the effect of nuclear deformation on proton bubble structure in $N = 28$ isotones. The theoretical calculations are carried out by using relativistic Hartree-Bogoliubov model based on density-dependent meson-exchange (DD-ME2) interaction. The isotones of $N = 28$ shell closure are known to exhibit a deformed ground state. Due to the weaking of spin-orbit strength, the $2s_{1/2}$-$1d_{3/2}$ states get inverted. We found that the central depletion of proton density in these isotones is greatly affected by nuclear deformation. The strong dynamical correlations, arising due to deformation, disfavors the bubble formation. The decrease in depletion

fraction can be related to increase in the central nucleon density (internal density) due to deformation. The study of deformed bubble structure and internal density is desired from an experimental perspective.

## Authorship Contribution

**Pankaj Kumar** Conceptualization, Investigation, Methodology, Resources, Visualization, Writing - original draft. **Virender Thakur:** Methodology, Resources, Writing - review & editing. **Smriti Thakur:** Resources, Writing - review & editing. **Raj Kumar:** Resources, Writing - review & editing, Supervision. **Shashi K. Dhiman:** Conceptualization, Methodology, Supervision, Validation.

## Conflict of Interest

The authors declare that they have no known competing financial interests or personal relationships that could have appeared to influence the work reported in this paper.

## Declaration

This is an original work and has neither been sent elsewhere nor published anywhere.

## References

[1] H. A. Wilson. *Physical Review,* **69**(9-10):538, (1946). https://doi.org/10.1103/PhysRev.69.538

[2] X. Campi and D. W. L. Sprung. *Physics Letters B,* **46**(3):291-295, (1973). https://doi.org/10.1016/0370-2693(73)90121-4

[3] J. M. Cavedon, B. Frois, D. Goutte, M. Huet, Ph Leconte, C. N. Papanicolas, X-H Phan, S. K. Platchkov, S. Williamson, W. Boeglin, et al. *Physical Review Letters,* **49**(14):978, 1982. https://doi.org/10.1103/PhysRevLett.49.978

[4] E. Khan, M. Grasso, J. Margueron, and Nguyen Van Giai, *Nuclear Physics A, 800*(1-4), 37-46 (2008). https://doi.Org/10.1016/j.nuclphysa.2007.ll.012

[5] M. Grasso, L. Gaudefroy, E. Khan, Tamara Niksic, J. Piekarewicz, O. Sorlin, Nguyen Van Giai, and Dario Vretenar, *Physical Review C, 79*(3), 034318 (2009). https://doi.org/10.1103/PhysRevC.79.034318

[6] Y. Z. Wang, J. Z. Gu, X. Z. Zhang, J. M. Dong, et al., *Physical Review C, 84*(4), 044333 (2011). https://doi.org/10.1103/PhysRevC.84.044333

[7] J. M. Yao, Hua Mei, and Z. P. Li, *Physics Letters B, 723*(4-5), 459-463 (2013). https://doi.Org/10.1016/j.physletb.2013.05.049

[8] T. Duguet, V. Soma, S. Lecluse, C. Barbieri, and P Navratil, *Physical Review* C, *95*(3), 034319 (2017). https://doi.org/10.1103/PhysRevC.95.034319

[9] G. Saxena, M. Kumawat, M. Kaushik, S. K. Jain, and Mamta Aggarwal, *Physics Letters B, 788*, 1-6 (2019). https://doi.Org/10.1016/j.physletb.2018.08.076

[10] J. Dechargé, J. -F. Berger, K. Dietrich, and M. S. Weiss, *Physics Letters B, 451*(3-4), 275-282 (1999). https://doi.org/10.1016/S0370-2693(99)00225-7

[11] A. V. Afanasjev and S. Frauendorf, *Physical Review C, 71*(2), 024308 (2005). https://doi:10.1103/PhysRevC.71.024308

[12] M. Bender and P-H Heenen, In *Journal of Physics: Conference Series, 420*, page 012002. IOP Publishing (2013). https://doi.Org/10.1088/1742-6596/420/l/012002

[13] A. Mutschler, A. Lemasson, O. Sorlin, D. Bazin, C. Borcea, R. Borcea, Z. Dombrádi, J-P Ebran, A Gade, H Iwasaki, et al., *Nature Physics, 13*(2), 152-156 (2017). https://doi.org/10.1038/nphys3916

[14] G. Saxena, M. Kumawat, B. K. Agrawal, and Mamta Aggarwal, *Physics Letters B, 789*, 323-328 (2019). https://doi.Org/10.1016/j.physletb.2018.10.062

[15] X. Y. Wu, J. M. Yao, Z. P. Li, et al., *Physical Review C, 89*(1), 017304 (2014). https://doi.org/10.1103/PhysRevC.89.017304

[16] A. Shukla and Sven Åberg, *Physical Review C, 89*(1), 014329 (2014). https://doi.org/10.1103/PhysRevC.89.014329

[17] P. Kumar, V. Thakur, V. Kumar, and S. K. Dhiman, *The European Physical Journal Plus, 136*(10), 1-11 (2021). https://doi.org/10.1140/epjp/sl3360-021-02036-0

[18] P. Kumar, V. Thakur, S. Thakur, V. Kumar, and S. K. Dhiman, *Acta Physica Polonica B, 52*(5) (2021). https://doi.org/10.5506/APhysPolB.52.401

[19] B. Schuetrumpf, W. Nazarewicz, and P-G Reinhard, *Physical Review C, 96*(2), 024306 (2017). https://doi.org/10.1103/PhysRevC.96.024306

[20] J Meng, H Toki, JY Zeng, SQ Zhang, and S-G Zhou, *Physical Review C, 65*(4), 041302 (2002). https://doi.org/10.1103/PhysRevC.65.041302

[21] P. Kumar, V. Thakur, S. Thakur, V. Kumar, and S. K. Dhiman, *The European Physical Journal A, 57*(1):1-13 (2021). https://doi.org/10.1140/epja/sl0050-021-00346-6

[22] G. A. Lalazissis, Tamara Niksic, Dario Vretenar, and Peter Ring, *Physical Review C, 71*(2), 024312 (2005). https://doi.org/10.1103/PhysRevC.71.024312

[23] G. A. Lalazissis, *Progress in Particle and Nuclear Physics, 59*, 277-284 (2007). https://doi.Org/10.1016/j.ppnp.2006.12.028

[24] S. Typel and H. H. Wolter, *Nuclear Physics A, 656* (3-4), 331-364 (1999). https://doi.org/10.1016/S0375-9474(99)00310-3

[25] F. Hofmann, C. M. Keil, and H. Lenske, *Physical Review C, 64*(3), 034314 (2001). https://doi.org/10.1103/PhysRevC.64.034314

[26] F. De Jong and H. Lenske, *Physical Review C, 57*(6), 3099 (1998). https://doi.org/10.1103/PhysRevC.57.3099

[27] Y. Tian, Zhong-Yu Ma, and P. Ring, *Physics Letters B, 676*(1-3), 44-50 (2009). https://doi.Org/10.1016/j.physletb.2009.04.067

[28] T. Nikšić, P. Ring, D. Vretenar, Y. Tian, and Zhong-yu Ma, *Physical Review C, 81*(5), 054318 (2010). https://doi.org/10.1103/PhysRevC.81.054318

[29] T. Nikšić, N. Paar, D. Vretenar, and P. Ring, *Computer physics communications, 185*(6), 1808-1821 (2014). https://doi.Org/10.1016/j.cpc.2014.02.027

[30] Y. Tian, Zhong-Yu Ma, and Peter Ring, *Physical Review C, 79*(6), 064301 (2009). https://doi.org/10.1103/PhysRevC.79.064301

[31] G. A. Lalazissis, Dario Vretenar, Peter Ring, M. Stoitsov, and L. M. Robledo, *Physical Review C, 60*(1), 014310 (1999). https://doi.org/10.1103/PhysRevC.60.014310

[32] O. Sorlin, *Nuclear Physics A, 834*(1-4), 400c-403c (2010). https://doi.Org/10.1016/j.nuclphysa.2010.01.049

[33] Z. P. Li, J. M. Yao, Dario Vretenar, Tamara Nikšić, H. Chen, and Jie Meng, *Physical Review C, 84*(5), 054304 (2011). https://doi.org/10.1103/PhysRevC.84.054304

[34] J. Dechargé, J. -F. Berger, M. Girod, and K. Dietrich, *Nuclear Physics A,* **716**, 55-86 (2003). https://doi.org/10.1016/S0375-9474(02)01398-2

[35] S. Raman, C.W. Nestor Jr., and P. Tikkanen, *Nuclear\ Data Tables* **78**, 1-128 (2001). https://doi.org/10.1006/adnd.2001.0858

[36] W. Horiuchi and T. Inakura, *Progress of Theoretical and Experimental Physics,* **2021**(10), 103D02 (2021). https://doi.org/10.1093/ptep/ptab087

**Journal of Nuclear Physics, Material Sciences, Radiation and Applications**